CRYSTAL GROWTH & DESIGN

Article

pubs.acs.org/crystal

Assembly of Polyoxometalate-Based Metal–Organic Frameworks with Silver(I)-Schiff Base Coordination Polymeric Chains as Building Blocks

Dongbin Dang, Yanning Zheng, Yan Bai,* Xiangyang Guo, Pengtao Ma, and Jingyang Niu*

Institute of Molecular and Crystal Engineering, School of Chemistry and Chemical Engineering, Henan University, Kaifeng, 475004, China

Supporting Information

ABSTRACT: Six crystalline polyoxometalate-based three-dimensional (3D) metal–organic frameworks $\{[AgL^4(DMF)][AgL^4]_2(PMo_{12}O_{40})\cdot DMF\cdot 3H_2O\}_n$ (**1**), $\{[AgL^4]_3(PW_{12}O_{40})\cdot 6H_2O\}_n$ (**2**), $\{[AgL^5]_3(PMo_{12}O_{40})\cdot (CH_3CN)_3\}_n$ (**3**), $\{[AgL^5(PW_{12}O_{40})][AgL^5(H_2O)_{0.25}(MeOH)_{0.25})][AgL^5]_{0.5}\cdot DMF\cdot (H_2O)_{1.5}\}_n$ (**4**), $\{[AgL^6]_3(PMo_{12}O_{40})\cdot DMF\cdot H_2O\}_n$ (**5**), and $\{[AgL^7]_3(PMo_{12}O_{40})\cdot DMF\cdot (CH_3CN)_3\}_n$ (**6**) have been successfully synthesized based on one-dimensional (1D) coordination polymers constructed by the coordination of polydentate Schiff-base ligands and silver cations and saturated α-Keggin polyoxoanion $[PM_{12}O_{40}]^{3-}$ (M = W, Mo) as building blocks, where L^4, L^5, L^6, and L^7 are 2,5-bis(3-pyridyl)-3,4-diaza-2,4-hexadiene, 1,4-bis(3-pyridyl)-2,3-diaza-1,3-butadiene, 2,5-bis(4-pyridyl)-3,4-diaza-2,4-hexadiene, and 1,4-bis-(4-pyridyl)-2,3-diaza-1,3-butadiene, respectively. Compounds **1**–**6** are structurally characterized by elemental analyses, IR spectroscopy, thermogravimetric analyses (TG), powder X-ray diffraction (XRD), and complete single-crystal X-ray diffraction analyses. The structures of **1**–**6** exhibit 3D supramolecular networks formed by linking 1D Ag-Schiff base chains and α-Keggin polyoxoanion units through the cooperativity of multiform supramolecular interactions, such as intermolecular Ag···O weak interactions, Ag···π interactions, π···π interactions, and hydrogen bonds. The photoluminescent properties of **1**–**6** have been investigated in the solid state.

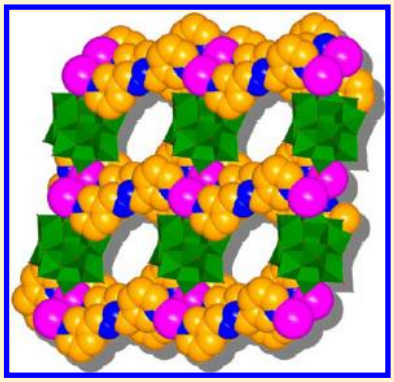

INTRODUCTION

Polyoxometalates (POMs) are regarded as one kind of outstanding inorganic building block for the design and synthesis of inorganic–organic hybrid materials due to the coordination ability of the numerous external oxygen atoms and attractive discrete, nanometer-sized, electronic and molecular properties.[1−4] One of the remarkable approaches in the design of functionalized materials based on POMs is to combine the POMs with transition-metal complexes (TMCs). This strategy is anticipated to obtain new POM-based compounds with a variety of structural motifs and interesting physical properties, which should lead to new molecular-framework materials.[5−7] More recently, a comprehensive library of POM-based networks incorporating electrophilic Ag(I) species have attracted considerable interest owing to silver's ability to form bonds with different donors simultaneously, a large radius, a wide variety of coordination geometries, and special photophysical and photochemical properties.[8−19] Some investigations have addressed the use of different organic ligands, such as 2,2′-bipy,[11,12] 4,4′-bipy,[11,13] 2,4′-bipy,[14] 1,10-phenathroline,[11,15] and fluconazole (1-(2,4-difluorophenyl)-1,1-bis[(1*H*-1,2,4-triazol-1-yl)methyl]ethanol (Hfcz)[16] for the preparation of a rich range of POM-based structures with Ag(I) ion. Apparently, the appropriate design of organic ligands is undoubtedly a key element in assembling POM/silver/ligand inorganic–organic hybrid compounds.

Polydentate Schiff base ligands with two pyridylimine sites connected by N–N single bonds are excellent ligands to generate interesting architectures.[20] However, there are only a few literature citations reported on the crystal engineering of POM species with Schiff base ligands,[18,19,21] even though Schiff base ligands are commonly used in metal–organic chemistry, owing to their ease of synthesis and high yield in a single-step reaction from commercially inexpensive reagents. As part of our studies on the construction of metal-Schiff base species and POM-based compounds,[17,22,23] our current interest is the incorporation of silver-Schiff base systems and POMs in these fascinating hybrid materials.[18,19]

In our latest report, successful attempts have been made to engineer POM-based silver compounds, such as three-dimensional (3D) porous crystalline arrays $[Ag_2L^1_2]_6(PMo_{12}O_{40})_4\cdot 5DMF\cdot 3H_2O$ and a double helicates bisupporting cluster $[(PMo_{12}O_{40})(Ag_2L^2_2)_2]OH\cdot 3H_2O$ based on silver(I) double helicates,[18] three POM-based hybrid compounds $\{[Ag_3L^3_3](PW_{12}O_{40})(CH_3CN)(DMF)_{2.5}\}_n$, $[Ag_4L^3_3(CH_3CN)_4][Ag_2L^3(CH_3CN)_3](PMo_{12}O_{40})_2\cdot CH_3CN$, and $[(SiMo_{12}O_{40})\{Ag_2L^3(CH_3CN)_3\}_2]\cdot (CH_3CN)_2$ based on silver(I)-L^3 species (Scheme 1).[19] Herein the chosen ligands, L^4, L^5, L^6, and L^7, are

Received: January 16, 2012
Revised: June 12, 2012
Published: June 14, 2012

Scheme 1. Schematic Drawing of Ligands L^1, L^2, L^3, L^4, L^5, L^6, and L^7

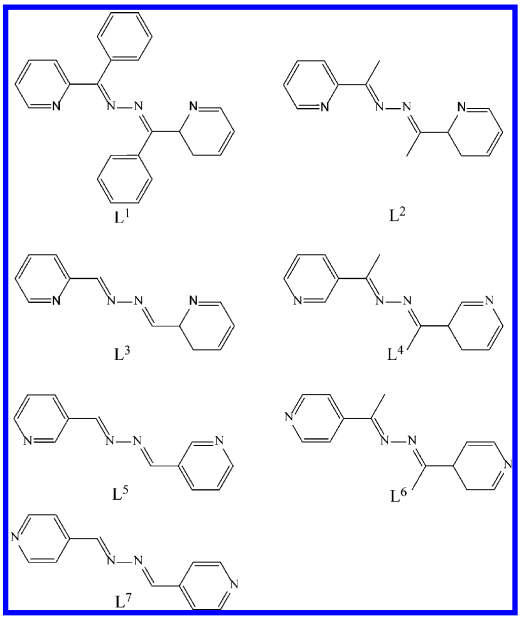

easy-to-prepare tailored derivatives of 4,4′-bipyridyl or 3,3′-bipyridyl ligands with a −CR═N−N═CR− spacer between the two pyridyl functions.[24,25] The most interesting feature was the nature of such type ligands themselves with their combination of weakly binding imine N donors and more strongly binding pyridyl N donors. Therefore, using ligands L^4, L^5, L^6, and L^7 to synthesize POM-based coordination polymers is particularly attractive given the following considerations: (i) The structure stabilization of silver coordination polymers based on these symmetrically bridged Schiff-base ligands provides access to assemble POM-based frameworks containing ligand-supported silver bridges.[26] (ii) Because the selected silver-Schiff base system is an anion-dependent species, the electrostatic interactions driven by the POM anions are an essential factor influencing molecular formation and crystallization. (iii) The long distance of two pyridyl N donors from a ligand provides a chance to create porous frameworks in the presence of the nanometer-sized POM anions. With these in mind, in this paper we report the synthesis and luminescent properties of six interesting 3D POM-based frameworks constructed from one-dimensional (1D) Ag-Schiff-base polymeric species and saturated Keggin type polyoxoanions $[PM_{12}O_{40}]^{3-}$ (M = W, Mo), including $\{[AgL^4(DMF)][AgL^4]_2(PMo_{12}O_{40})\cdot DMF\cdot 3H_2O\}_n$ (**1**), $\{[(AgL^4)_3](PW_{12}O_{40})\cdot 6H_2O\}_n$ (**2**), $\{[AgL^5]_3(PMo_{12}O_{40})\cdot(CH_3CN)_3\}_n$ (**3**), $\{[AgL^5(PW_{12}O_{40})][AgL^5(H_2O)_{0.25}(MeOH)_{0.25})][AgL^5]_{0.5}DMF\cdot(H_2O)_{1.5}\}_n$ (**4**), $\{[AgL^6]_3(PMo_{12}O_{40})\cdot\cdot DMF\cdot H_2O\}_n$ (**5**), and $\{[AgL^7]_3(PMo_{12}O_{40})\cdot DMF\cdot\cdot(CH_3CN)_3\}_n$ (**6**).

EXPERIMENTAL SECTION

Materials. All reagents were used as purchased without further purification. Ligands L^4, L^5, L^6, and L^7 were synthesized by a previously reported procedure and were extensively characterized.[24] $H_3PMo_{12}O_{40}\cdot xH_2O$ and $H_3PW_{12}O_{40}\cdot xH_2O$ were synthesized as described in ref 27.

General Characterization and Physical Measurements. Elemental analyses (C, H, and N) were performed on a Perkin-Elmer 2400-II CHNS/O analyzer. Elemental analyses (P, W, Mo, and Ag) were determined by a Perkin-Elmer Optima 2100DV inductively coupled plasma-optical emission spectrometer. IR spectra were recorded on a Nicolet 360 FT-IR spectrometer using KBr pellets in the range of 4000−400 cm^{-1}. Thermogravimetric (TG) analyses were carried out on a Perkin-Elmer-7 thermal analyzer in the temperature region of 25−800 °C with a heating rate of 10 °C·min^{-1}, and the luminescent spectra were recorded on a HITACHI F-7000 fluorescence spectrophotometer. N_2 adsorption was measured on an ASAP 2020 gas-adsorption apparatus at liquid-nitrogen (77 K) temperature. The crystalline samples of the compounds were identified by powder X-ray diffraction (XRD) using a Philips X'Pert Pro Super diffractometer with graphite monochromatized Cu Kα radiation (λ = 1.541 78 Å).

Synthesis of $\{[AgL^4(DMF)][AgL^4]_2(PMo_{12}O_{40})\cdot DMF\cdot 3H_2O\}_n$ (1). A solution of L^4 (0.012 g, 0.05 mmol) in CH_3CN (6 mL) was slowly layered onto a solution of $H_3PMo_{12}O_{40}\cdot xH_2O$ (0.10 g) and $AgNO_3$ (0.025 g, 0.15 mmol) in DMF (4 mL). The solutions were left in darkness at room temperature for two weeks to give yellow block crystals in 42% yields (based on $H_3PMo_{12}O_{40}\cdot xH_2O$). Anal. Calcd. (found %) for $C_{48}H_{62}N_{14}Ag_3PMo_{12}O_{45}$: C 18.83 (18.49). H 2.04 (2.20). N 6.41 (6.26). P 1.01 (1.10). Mo 37.61 (36.90). Ag 10.57 (10.50). IR (cm^{-1}, KBr pellet): 3445(w), 1654(m), 1615(s), 1474(w), 1421(w), 1384(w), 1366(w), 1308(w), 1297(w), 1197(w), 1061(vs), 956(vs), 877(s), 807(vs), 798(vs), 697(s), 668(w), 504(m).

Synthesis of $\{[(AgL^4)_3](PW_{12}O_{40})\cdot 6H_2O\}_n$ (2). The reaction procedure was carried out in a similar manner to that of **1**, except that $H_3PW_{12}O_{40}\cdot xH_2O$ (0.10 g) was used instead of $H_3PMo_{12}O_{40}\cdot xH_2O$ (0.10 g). The product, **2**, was obtained in 30% yield (based on $H_3PW_{12}O_{40}\cdot xH_2O$). Anal. Calcd. (found %) for $C_{42}H_{54}N_{12}Ag_3PW_{12}O_{46}$: C 12.54 (12.68). H 1.35 (1.18). N 4.18 (4.31). P 0.77 (0.80). W 54.86 (55.10). Ag 8.04 (8.02). IR (cm^{-1}, KBr pellet): 3460(m), 1652(vs), 1616(m), 1474(w), 1425(m), 1368(m) 1384(w), 1296(w), 1252(w), 1199(m), 1079(vs), 977(vs), 894(vs), 877(s), 822(s), 697(s), 595(w), 510(m).

Synthesis of $\{[AgL^5]_3(PMo_{12}O_{40})\cdot(CH_3CN)_3\}_n$ (3). The reaction procedure was carried out in a similar manner to that of **1**, except that L^5 (0.010 g, 0.05 mmol) was used instead of L^4 (0.012 g, 0.05 mmol). The product, **3**, was obtained in 38% yield (based on $H_3PMo_{12}O_{40}\cdot xH_2O$). Anal. Calcd. (found %) for $C_{42}H_{39}N_{15}Ag_3PMo_{12}O_{40}$: C 17.40 (17.32). H 1.36 (1.44). N 7.25 (7.12). P 1.07 (1.01). Mo 39.70 (39.50). Ag 11.16 (11.08). IR (cm^{-1}, KBr pellet): 3444(w), 1655(m), 1628(m), 1423(m), 1384(w), 1308(w), 1194(w), 1062(vs), 961(vs), 874(s), 817(s), 695(s), 653(w), 617(w), 504(m).

Synthesis of $\{[AgL^5(PW_{12}O_{40})][AgL^5(H_2O)_{0.25}(MeOH)_{0.25})][AgL^5]_{0.5}\cdot DMF\cdot(H_2O)_{1.5}\}_n$ (4). Ligand L^5 (0.010 g, 0.05 mmol) was stirred in methanol solution (6 mL) and was slowly layered onto a solution of $H_3PW_{12}O_{40}\cdot xH_2O$ (0.10 g) and $AgNO_3$ (0.025 g, 0.15 mmol) in DMF (4 mL). The solutions were left for two weeks at room temperature in darkness to give X-ray quality yellow block crystals in 27% yields (based on $H_3PW_{12}O_{40}\cdot xH_2O$). Anal. Calcd. (found %) for $C_{33.25}H_{36.5}N_{11}Ag_{2.5}PW_{12}O_{43}$: C 10.55 (10.70). H 0.96 (1.04). N 4.07 (4.15). P 0.82 (0.85). W 58.29 (58.40). Ag 7.12 (7.15). IR (cm^{-1}, KBr pellet): 3452(w), 1655(m), 1628(m), 1423(m), 1384(w), 1325(w), 1308(w), 1079(vs), 976(vs), 894(s), 804(vs), 696(s), 660(w), 591(w), 519(m).

Synthesis of $\{[AgL^6]_3(PMo_{12}O_{40})\cdot DMF\cdot H_2O\}_n$ (5). The reaction procedure was carried out in a similar manner to that of **1**, except that L^6 (0.012 g, 0.05 mmol) was used instead of L^4 (0.012 g, 0.05 mmol). The product, **5**, was obtained in 37% yield (based on $H_3PMo_{12}O_{40}\cdot xH_2O$). Anal. Calcd. (found %) for $C_{45}H_{51}N_{13}Ag_3PMo_{12}O_{42}$: C 18.31 (18.43). H 1.74 (1.65). N 6.17 (6.10). P 1.05 (1.02). Mo 39.00 (38.85). Ag 10.96 (11.05). IR (cm^{-1}, KBr pellet): 3445(w), 1652(m), 1608(s), 1540(w), 1496(w), 1419(m), 1384(w), 1368(w), 1326(w), 1289(w), 1101(w), 1060(vs), 953(vs), 791(vs), 665(w), 642(w), 577(w), 502(w).

Synthesis of $\{[AgL^7]_3(PMo_{12}O_{40})\cdot DMF\cdot(CH_3CN)_3\}_n$ (6). The reaction procedure was carried out in a similar manner to that of **1**, except that L^7 (0.010 g, 0.05 mmol) was used instead of L^4 (0.012 g, 0.05 mmol). The product, **6**, was obtained in 46% yield (based on

dx.doi.org/10.1021/cg300075a | Cryst. Growth Des. 2012, 12, 3856−3867

Table 1. Crystallographic Data and Structural Refinements for 1−6

	1	2	3	4	5	6
formula	$C_{48}H_{62}N_{14}Ag_3PMo_{12}O_{45}$	$C_{42}H_{54}N_{12}Ag_3PW_{12}O_{46}$	$C_{42}H_{39}N_{15}Ag_3PMo_{12}O_{40}$	$C_{33.25}H_{36.5}N_{11}Ag_{2.5}PW_{12}O_{43}$	$C_{45}H_{51}N_{13}Ag_3PMo_{12}O_{42}$	$C_{45}H_{46}N_{16}Ag_3PMo_{12}O_{41}$
M_r (g mol^{-1})	3060.98	4023.75	2899.74	3785.08	2951.78	2972.84
T (K)	296(2)	296(2)	273(2)	273(2)	296(2)	273(2)
space group	$P2_1$	$P2_1$	$P\bar{1}$	$P\bar{1}$	$P\bar{1}$	$P\bar{1}$
crystal system	monoclinic	monoclinic	triclinic	triclinic	triclinic	triclinic
a (Å)	12.259(2)	12.1944(16)	11.6621(9)	14.2253(7)	12.1185(12)	12.1046(2)
b (Å)	20.215(4)	20.2254(13)	13.4355(11)	15.6220(8)	13.7109(13)	12.9993(2)
c (Å)	17.619(4)	17.5747(11)	13.9027(10)	17.6383(9)	14.0587(14)	14.1836(2)
α (deg)			76.274(5)	90.988(4)	73.451(2)	105.0890(10)
β (deg)	97.105(4)	96.757(2)	67.563(5)	95.278(3)	82.619(2)	90.2270(10)
γ (deg)			69.521(3)	92.213(3)	73.220(2)	102.7890(10)
V (Å^3)	4332.5(15)	4304.5(5)	1872.6(3)	3899.3(3)	2141.1(4)	2096.90(6)
Z	2	2	1	2	1	1
D_c (g cm^{-3})	2.346	4.091	2.571	3.224	2.282	2.354
μ (mm^{-1})	2.447	22.795	2.819	18.338	2.469	2.522
limiting indices	$-14 \le h \le 10$	$-13 \le h \le 14$	$-13 \le h \le 13$	$-16 \le h \le 16$	$-14 \le h \le 14$	$-14 \le h \le 14$
	$-24 \le k \le 23$	$-24 \le k \le 24$	$-15 \le k \le 15$	$-18 \le k \le 17$	$-16 \le k \le 11$	$-15 \le k \le 15$
	$-20 \le l \le 19$	$-16 \le l \le 20$	$-16 \le l \le 16$	$-20 \le l \le 20$	$-16 \le l \le 14$	$-14 \le l \le 17$
GOF on F^2	1.082	1.035	1.084	1.012	1.176	1.061
R_1, wR_2 [$I > 2\sigma(I)$]	0.0899, 0.1594	0.0536, 0.1076	0.0855, 0.1899	0.059, 0.1293	0.0706, 0.1609	0.0465, 0.1132
R_1, wR_2 [all data]	0.1907, 0.1830	0.1045, 0.1203	0.1150, 0.1998	0.1431, 0.1494	0.0850, 0.1652	0.0692, 0.1238

dx.doi.org/10.1021/cg300075a | Cryst. Growth Des. 2012, 12, 3856−3867

$H_3PMo_{12}O_{40}\cdot xH_2O$). Anal. Calcd. (found %) for $C_{45}H_{46}N_{16}Ag_3PMo_{12}O_{41}$: C 18.18 (18.26). H 1.56 (1.47). N 7.54 (7.48). P 1.04 (0.99). Mo 38.73 (38.78). Ag 10.89 (10.72). IR (cm^{-1}, KBr pellet): 3453(w), 1652(m), 1557(w), 1505(w), 1413(m), 1384(w), 1255(w), 1106(w), 1062(vs), 957(vs), 882(vs), 803(s), 625(w), 537(w), 515(w).

X-ray Crystallography. X-ray single crystal diffraction data for compounds **1**−**6** were collected on a Bruker Apex-II CCD detector using graphite monochromatized Mo−Kα radiation (λ = 0.71073 Å) at room temperature. Routine Lorentz and polarization corrections were applied. The structures were solved by direct method of SHELXS-97[28] and refined by full-matrix least-squares method using the SHELXL-97 program package.[29] All of the non-hydrogen atoms except the disordered solvent molecules were refined with anisotropic thermal displacement coefficients. Hydrogen atoms were assigned to calculated positions using a riding model with appropriately fixed isotropic thermal parameters. The detailed crystallographic data and structure refinement parameters are summarized in Table 1. Selected bond distances, bond angles, and hydrogen bonding interactions for compounds **1**−**6** are listed in Tables S1−S18 (Supporting Information).

RESULTS AND DISCUSSION

Structure Description of 1. The compound **1** crystallizes in the monoclinic space group $P2_1$. Single-crystal X-ray diffraction analysis revealed that the structure of **1** exhibits a crystalline 3D chiral MOF constructed by 1D silver coordination polymeric cations and $[PMo_{12}O_{40}]^{3-}$ anions as building blocks. There are three types of 1D Ag-L^4-chains and each contains one crystallographically independent silver(I) center (Figure 1a and Figure S1 in the Supporting Information). The Ag(1) atom is surrounded by two terminal $N_{pyridyl}$ atoms from two ligands [Ag(1)−N(1), 2.164(9) Å; Ag(1)−N(4A), 2.181(10) Å (symmetric code A: 1 + x, y, z)] and one oxygen atom from DMF [Ag(1)−O(41), 2.594(8) Å] to attain a distorted T-type geometry environment with the bond angle of 173.0(3)° for N(1)−Ag(1)−N(4A). Ag(2) and Ag(3) centers have similar coordination environments with two terminal $N_{pyridyl}$ atoms from two ligands coordination to one metal center, respectively. The bond angles are 173.7(4)° for N(5)−Ag(2)−N(8A) and 179.3(5)° for N(9)−Ag(3)−N-(12A). The average Ag−N distance in compound **1** is 2.17 Å. Adjacent Ag centers are bridged by each bis-monodentate ligand (two terminal $N_{pyridyl}$ donors) with the Ag···Ag separation of 12.3 Å to form three types of 1D chain structures [Ag(1)-L^4-chain, Ag(2)-L^4-chain, and Ag(3)-L^4-chain], respectively. Otherwise, six types of intramolecular C−H···N hydrogen bonds between carbon atoms of the CH_3 groups, the pyridyl groups, and imine N atoms play an important role in stabilizing the Ag(1)-L^4-chain and Ag(3)-L^4-chain structures.

The weak Ag···O interaction is found between Ag(1) and the oxygen atom O(5) of $[PMo_{12}O_{40}]^{3-}$ anion with the Ag(1)···O(5) distance of 3.00 Å. The adjacent Ag(2)-L^4-chain and Ag(1)-L^4-chain further interact with each other with weak Ag···N interaction (Ag···N distance: 2.85 Å) between the silver atom Ag(2) and the N_{imine} donor N(3) of Ag(1)-L^4-chain. Furthermore, there are two kinds of weak Ag···O interactions between Ag(3) and two oxygen atoms (O(8) from $[PMo_{12}O_{40}]^{3-}$ anion and O(42) from DMF molecule). The Ag···O distance is 2.84 Å for Ag(3)···O(42) and 2.95 Å for Ag(3)···O(8), respectively. Accordingly, each $[PMo_{12}O_{40}]^{3-}$ anion acts as a 2-connected node to link Ag(1) and Ag(3) atoms from the Ag(1)-L^4-chain and Ag(3)-L^4-chain, respectively. Detailed structural analyses revealed that the presence of the above weak interactions leads to the formation of an interesting 1D supramolecular structure. And the 1D structures were further interconnected to each other to form a two-dimensional (2D) supramolecular network through Ag···π interaction between the Ag(2) atom and pyridyl ring [N(9)C(29)−C(3)] of the Ag(3)-L^4-chain with the Ag(2)···Py distance of 3.54 Å. In addition, multiform types of C−H···N and C−H···O hydrogen bonds are found in the solid state and play an important role in forming and stabilizing the 3D supramolecular network (Figure 1b and Figure S2).

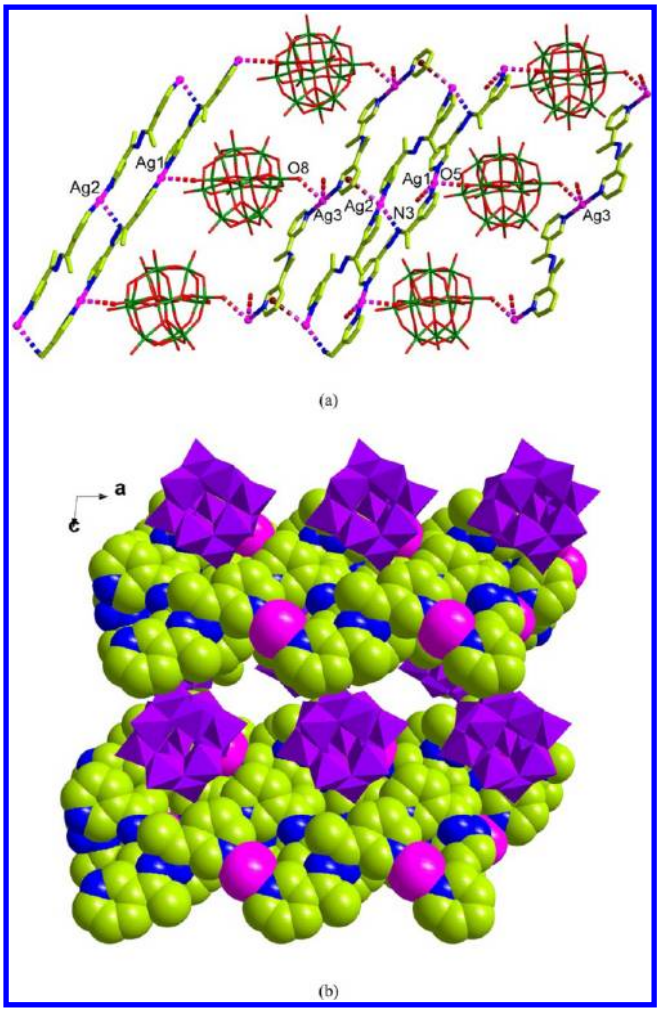

Figure 1. (a) A view of the 2D sheet based on three types of Ag-L^4 chains and $[PMo_{12}O_{40}]^{3-}$ anions in **1** showing weak Ag···O interactions, weak Ag···N interactions, and Ag···π interactions in dashed lines. (b) A view of the 3D supramolecular network of **1**.

Structure Description of 2. The compound **2** crystallizes in the $P2_1$ space group of the monoclinic system just as that of compound **1**. The asymmetry unit consists of one $[PW_{12}O_{40}]^{3-}$ anion, three $[AgL^4]^+$ units, and six disordered H_2O molecules (Figure S3). Each Ag(I) is bound to two terminal $N_{pyridyl}$ atoms from two ligands, and each ligand acts as a bidentate ligand to link two symmetrical Ag(1), Ag(2), or Ag(3) ions to form three types of 1D structures [Ag(1)-L^4-chain, Ag(2)-L^4-chain, and Ag(3)-L^4-chain] with the Ag···Ag separation of 12.19 Å (Figure 2a). The average Ag−$N_{pyridyl}$ distance is 2.14 Å. There are four types of C−H···N intramolecular hydrogen bonds which play an important role in stabilizing the Ag-L-chain structures. Two of them are between the CH_3 group and imine N atom of the ligand in the Ag(1)-L^4-chain and Ag(2)-L^4-chain. The other

dx.doi.org/10.1021/cg300075a | Cryst. Growth Des. 2012, 12, 3856−3867

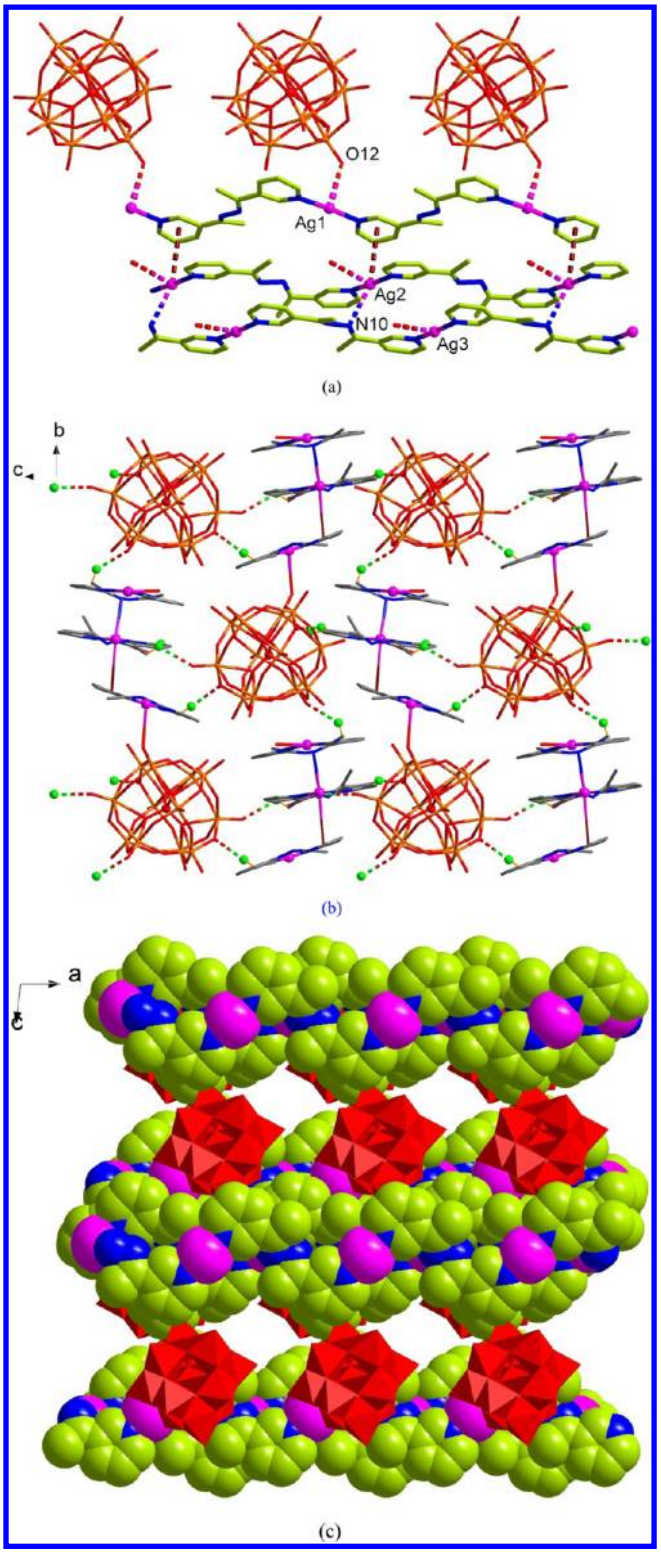

Figure 2. (a) A view of the 1D structure based on three types of Ag-L^4 chains and $[PW_{12}O_{40}]^{3-}$ anions in **2** showing weak Ag···O interactions, weak Ag···N interactions, and Ag···π interactions in dashed lines. (b) A view of the 3D supramolecular network along the *bc* plane in **2** showing hydrogen bonds in dashed lines. (c) A view of the 3D supramolecular network along the *ac* plane in **2**.

two are found between the pyridyl group and the imine N atom of the ligand in the Ag(3)-L^4-chain structure.

Interestingly, there are multiform weak interactions between silver centers and adjacent units besides two Ag−N coordination bonds. The weak Ag···O interaction between Ag(1) and O(12) from the $[PW_{12}O_{40}]^{3-}$ anion is found with the distance of 2.94 Å. There is one type of Ag···π interaction between the Ag(2) atom and the pyridyl ring [N(4)C(10)−C(14)] of the Ag(1)-L^4-chain with the Ag(2)···Py distance of 3.50 Å. Weak Ag···N interaction (Ag···N distance: 2.91 Å) is found between Ag(2) and the N_{imine} donor N(10) of the Ag(3)-L^4-chain. Otherwise, there are two types of weak Ag···O interactions between Ag and H_2O with the distance of 3.02 Å for Ag(2)···O(2W) and 2.80 Å for Ag(3)···O(3W), respectively. Such Ag···O interactions, Ag···N interactions, and Ag···π interactions link three 1D polymer chains to form a 1D triple-chain supported $[PW_{12}O_{40}]^{3-}$ anions structure. Each 1D triple-strand structure as a subunit interconnects with adjacent six subunits through five types of C−H···O hydrogen bonds to form a 3D network in which each $[PW_{12}O_{40}]^{3-}$ anion offers six oxygen atoms as hydrogen acceptors (Figure 2b,c).

Structure Description of 3. X-ray diffraction analysis reveals that compound **3** exhibits a 3D network constructed from two types of 1D Ag Schiff-base chains and $[PMo_{12}O_{40}]^{3-}$ anions. Compound **3** crystallizes in a centrosymmetric space group $P\bar{1}$, and consequently there are one-half $[PMo_{12}O_{40}]^{3-}$ anion with the P atom lying at the symmetric center, one $[AgL^5]^+$ unit, one $[AgL^5]^+_{0.5}$ unit, and 1.5 CH_3CN molecules (Figure S4). Each ligand acts as a bidentate ligand linking two symmetrical Ag(1) or Ag(2) ions through two terminal $N_{pyridyl}$ atoms to form two types of 1D structures [Ag(1)-L^5-chain and Ag(2)-L^5-chain] with the Ag···Ag separation of 14.38 Å. The average Ag−$N_{pyridyl}$ distance is 2.15 Å.

As shown in Figure 3a, each $[PMo_{12}O_{40}]^{3-}$ anion interconnects with four Ag(1) centers from four Ag(1)-L^5-chain units through two symmetrical terminal oxygen atoms μ−O(3) with the Ag···O distance of 2.77 Å and 2.97 Å. Two Ag(1) atoms from a pair of Ag(1)-chain units are linked by two terminal oxygen atoms from two $[PMo_{12}O_{40}]^{3-}$ anions to form a four-membered ring. The Ag···Ag separation of 3.46 Å is only 0.02 Å longer than 3.44 Å (the sum of the van der Walls radii of two silver atoms). The cooperativity of above Ag(1)−N bonds and weak Ag···O interactions serve to increase the dimensionality of the compound to form a 2D sheet. It is interesting to note that there is obvious π···π interaction involving pyridyl rings of adjacent Ag(1)-L^5-chain units. The π···π interaction is characterized by the shortest interplanar atom···atom separation of 3.35 Å, the centroid···centroid separation of 3.84 Å, and the dihedral angle of 10.6°. The Ag(2)-L^5-chain units are fitted into the regions between the 2D sheets with two types of Ag···π interactions with the distances of 3.36 Å for Ag(1)···Py[N(5)-C(13)−C(17)] and 3.44 Å for Ag(2)···Py[N(4)C(8)−C(12)], respectively (Figure 3b). Such Ag···O interactions, π···π interactions, Ag···π interactions, and hydrogen bonds link the 1D polymeric chains to form a 3D structure (Figure 3c).

Structure Description of 4. X-ray diffraction analysis reveals that **4** exhibits a 3D network constructed from three types of 1D Ag Schiff-base chains and $[PW_{12}O_{40}]^{3-}$ anions. There are four crystallographically independent silver(I) centers (Figure S5). As shown in Figure 4a, Ag(1) is coordinated to two $N_{pyridyl}$ atoms from two ligands and one terminal oxygen atom O(10) from one $[PW_{12}O_{40}]^{3-}$ anion to attain a distorted T-type environment with the bond angle of 177.6(5)° for N(1)−Ag(1)−N(4). The presence of two weak Ag···O interactions between the Ag(1) atom and two oxygen

dx.doi.org/10.1021/cg300075a | *Cryst. Growth Des.* 2012, 12, 3856−3867

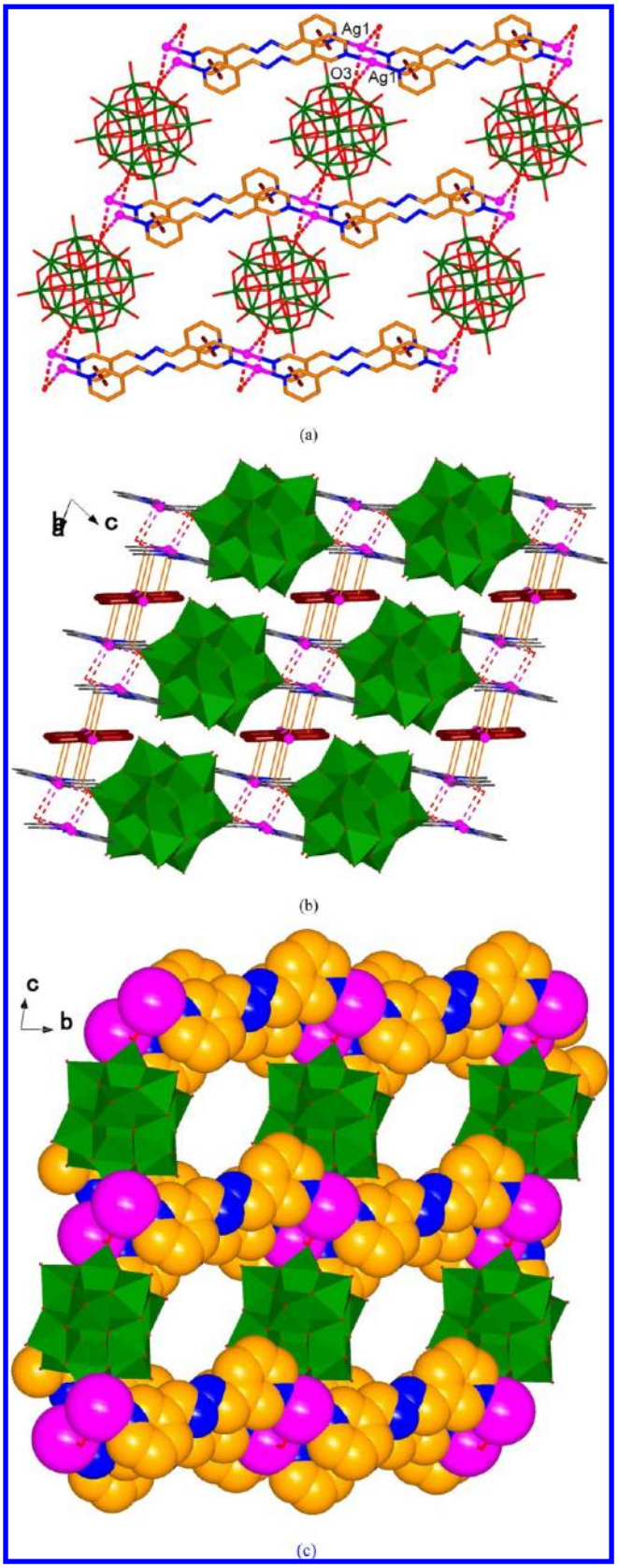

Figure 3. (a) A view of the 2D structure based on Ag(1)-L^5-chains and $[PMo_{12}O_{40}]^{3-}$ anions in **3** showing weak Ag···O interactions in dashed lines and $\pi\cdots\pi$ interactions in solid lines. (b) A view of the 3D supramolecular network in **3** showing Ag···O interactions in dashed lines and Ag···π interactions in solid lines. (c) A view of the 3D supramolecular network along the *bc* plane in **3**.

atoms O(6) from the $[PW_{12}O_{40}]^{3-}$ anion, O(1W) from the water molecule was an important influence on the coordination geometry of the Ag(1) center with the Ag···O distances of 2.73 Å and 2.82 Å, respectively. Adjacent Ag(1) centers are bridged by bis-monodentate ligand (two terminal $N_{pyridyl}$ donors) to form a 1D Ag(1)-L^2-chain structure supported $[PW_{12}O_{40}]^{3-}$ anions. Ag(2) is surrounded by two terminal $N_{pyridyl}$ atoms of two ligands with the bond angle of 174.7(5)° for N(5)−Ag(2)−N(8) (Figure 4b). Ag(3) is bound to one N_{imine} donor N(6) of ligand [Ag(3)−N(6) 2.383(16) Å], O(42) of MeOH [Ag(3)−O(42) 2.07(4) Å], and O(4W) of H_2O [Ag(3)−O(4W) 2.645(4) Å]. Therefore, one ligand acts as a tridentate ligand to link three silver(I) atoms [Ag(2), Ag(3), and Ag(2)] through two terminal $N_{pyridyl}$ and one N_{imine} donors with the Ag(2)···Ag(3) distance of 7.7 Å and the Ag(2)···Ag(2) distance of 14.23 Å. There are two kinds of weak Ag···O interactions between Ag(2) and two oxygen atoms O(8) from $[PW_{12}O_{40}]^{3-}$ anion, O(44) from DMF molecule, respectively. The Ag···O distance is 2.72 Å for Ag(2)···O(8) and 2.82 Å for Ag(2)···O(44). One type of weak Ag···O interaction between Ag(3) and O(12) from the $[PW_{12}O_{40}]^{3-}$ anion is found with the distance of 2.87 Å. As shown in Figure 4c, Ag(4) is coordinated to two terminal $N_{pyridyl}$ atoms from two ligands, and each ligand links two Ag(4) atoms to form a 1D Ag(4)-L^2-chain structure. Otherwise, Ag(4) interconnects with two oxygen atoms O(28) from two $[PW_{12}O_{40}]^{3-}$ anions with the Ag···O distance of 2.94 Å. The average Ag−$N_{pyridyl}$ distance is 2.16 Å.

In the solid state, each $[PW_{12}O_{40}]^{3-}$ anion acts as a 5-connected node to link five silver(I) centers through four terminal oxygen atoms and one bridging oxygen atom (Figure 4d). The existence of multiform Ag···O weak interactions between 1D chains and $[PW_{12}O_{40}]^{3-}$ anions gives further rise to a 2D network (Figure 4e). In addition, $\pi\cdots\pi$ interactions are found between pyridyl rings [N(1)C(1)−C(5)] of Ag(1)-L^2-chain and [N(9)C(25)−C(29)] of Ag(4)-L^2-chain and also play an important role in stabling the network. $\pi\cdots\pi$ interaction is characterized by the shortest interplanar atom···atom separation of 3.43 Å, the centroid···centroid separation of 3.91 Å, and the dihedral angle of 5.9°. A set of C−H···O hydrogen bonds are found to stabilize the supramolecular network (Figure 4f).

Structure Description of 5. Single-crystal X-ray diffraction analysis revealed that the structure of **5** exhibits a 3D supramolecular network based on two types of 1D polymeric chains and $[PMo_{12}O_{40}]^{3-}$ anions (Figure 5a and Figure S6). As shown in Figure 5b, through two terminal $N_{pyridyl}$ atoms, each ligand acts as a bidentate ligand to link two symmetrical Ag(1) or Ag(2) ions to form two similar 1D structures [Ag(1)-L^6-chain and Ag(2)-L^6-chain] with the Ag···Ag separation of 15.46 Å. The average Ag−$N_{pyridyl}$ distance is 2.13 Å. Two types of C−H···N intramolecular hydrogen bonds between the CH_3 groups and imine N atoms in the ligands play an important role in stabilizing the Ag(1)-L^6-chain structure.

The weak Ag···O interactions between Ag(1) and two oxygen atoms, O(1) from $[PMo_{12}O_{40}]^{3-}$ anion and O(23) [O(23′)] from disordered DMF molecule, are found with the distances of 2.72 Å for Ag(1)···O(1), 2.79 Å (2.76 Å) for Ag(1)···O(23) [O(23′)], respectively. For Ag(2), the two oxygen atoms from two symmetrical $[PMo_{12}O_{40}]^{3-}$ anions show long-range interactions with the Ag(2)···O(1) distance of 3.02 Å. Consequently, each terminal oxygen atom O(1) of

dx.doi.org/10.1021/cg300075a | *Cryst. Growth Des.* 2012, 12, 3856−3867

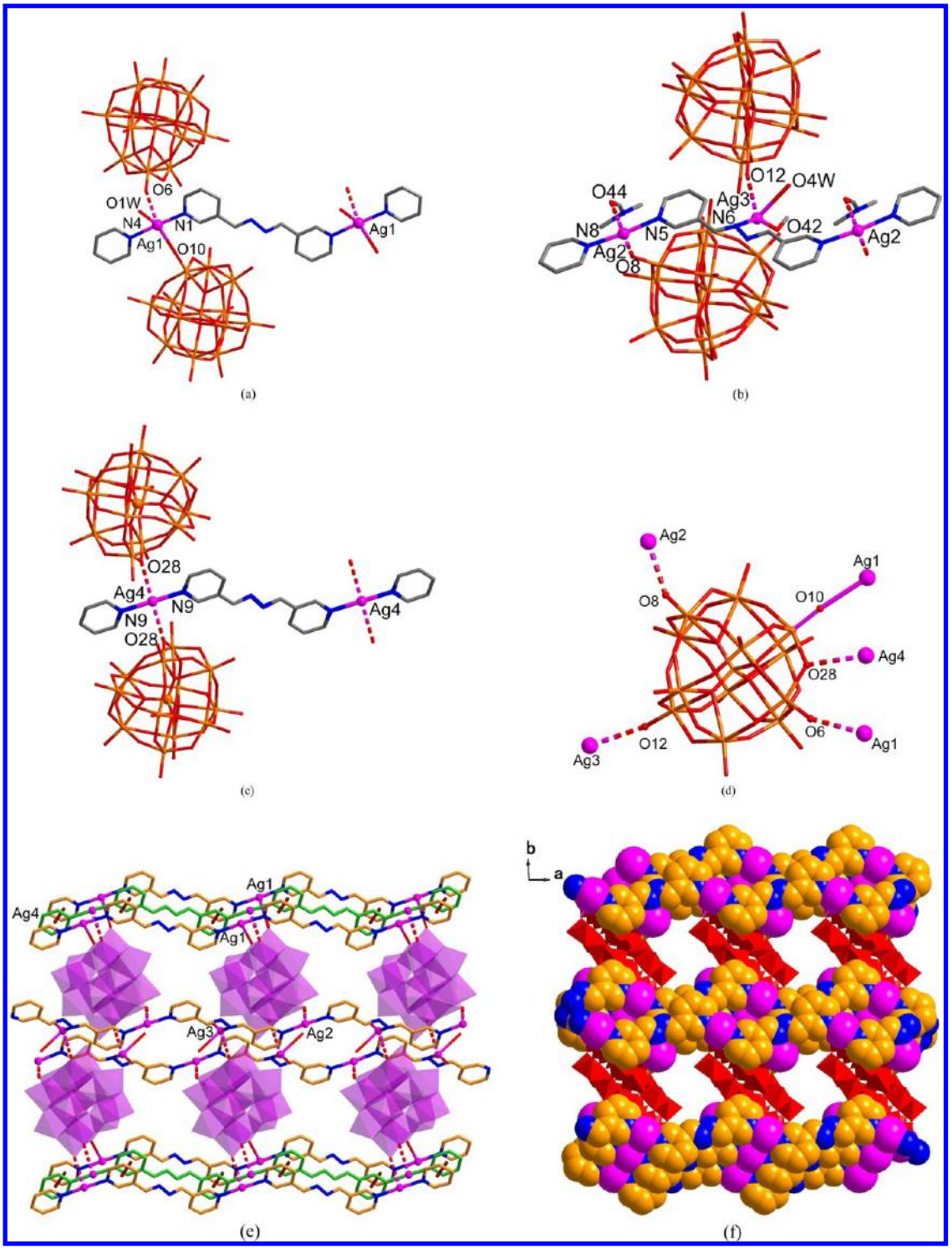

Figure 4. (a) A view of the coordination environment for Ag(1). (b) A view of the coordination environments for Ag(2) and Ag(3). (c) A view of the coordination environment for Ag(4). (d) A view of the coordination environment for $[PW_{12}O_{40}]^{3-}$ anion. (e) A view of 2D structure based on three types of 1D chains and $[PW_{12}O_{40}]^{3-}$ anions in **4** showing weak Ag···O interactions in dashed lines and $\pi\cdots\pi$ interactions in solid lines. (f) A view of the 3D supramolecular network along the *ab* plane in **4**.

$[PMo_{12}O_{40}]^{3-}$ anion links two silver(I) atoms Ag(1) and Ag(2) with the Ag(1)···Ag(2) distance of 3.71 Å. Such Ag···O weak interactions link the adjacent Ag(1)-L^6-chain, Ag(2)-L^6-chain, and $[PMo_{12}O_{40}]^{3-}$ units to form a 2D network. In additional, there are multiform C−H···O hydrogen bonds and obvious two types of $\pi\cdots\pi$ interactions involving pyridyl rings of adjacent Ag(1)-L^6-chain and Ag(2)-L^6-chain structures (Figure 5c and Figure S7). The shortest interplanar atom···atom separations, the centroid···centroid separations, and the dihedral angles are 3.40 Å (3.62 Å, 3.4°) and 3.46 Å (3.79 Å, 5.8°), respectively.

Structure Description of 6. The structure of compound **6** is similar to that found for compound **3** and exhibits a crystalline 3D structure based on two types of 1D Ag-L^7-chain units and $[PMo_{12}O_{40}]^{3-}$ anions as building blocks (Figure S8).

dx.doi.org/10.1021/cg300075a | *Cryst. Growth Des.* 2012, 12, 3856−3867

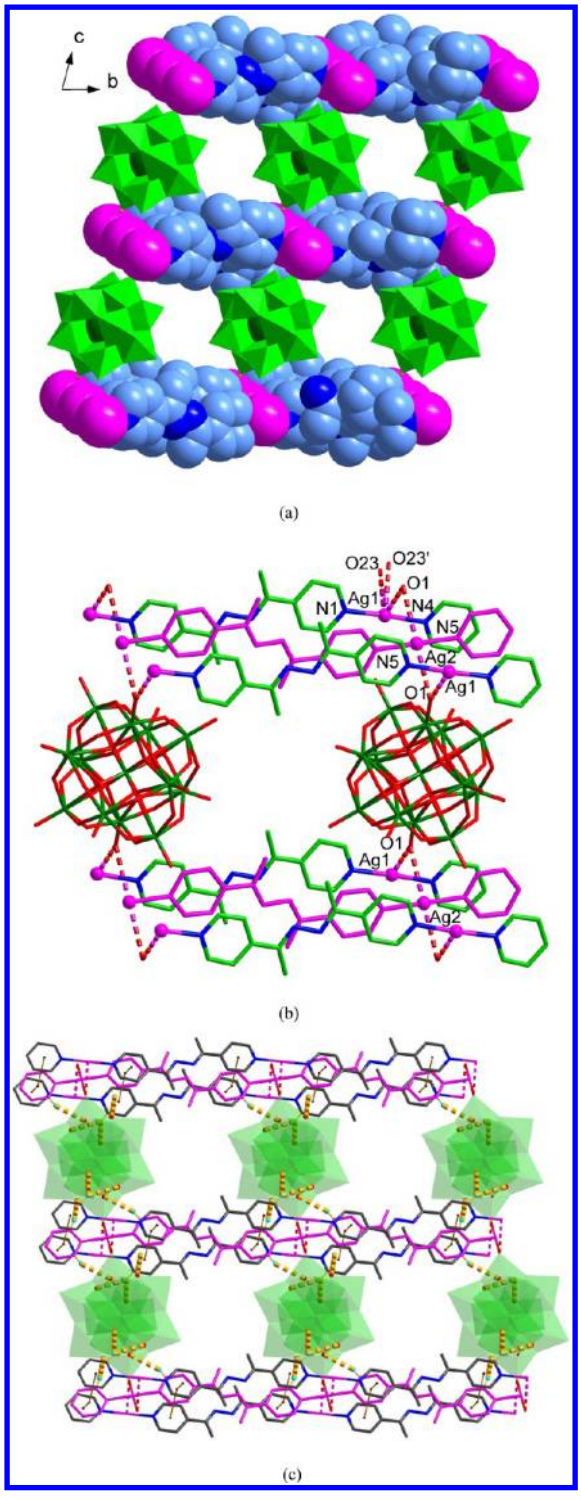

Figure 5. (a) A view of the 3D supramolecular network along the *bc* and *ac* planes in **5**. (b) A view of the environments for Ag(1) and Ag(2) atoms in **5** showing weak Ag···O interactions in dashed lines. (c) A view of the 2D structure based on two types of 1D chains and $[PMo_{12}O_{40}]^{3-}$ anions in **5** showing weak Ag···O interactions and C–H···O hydrogen bonds in dashed lines and $\pi\cdots\pi$ interactions in solid lines.

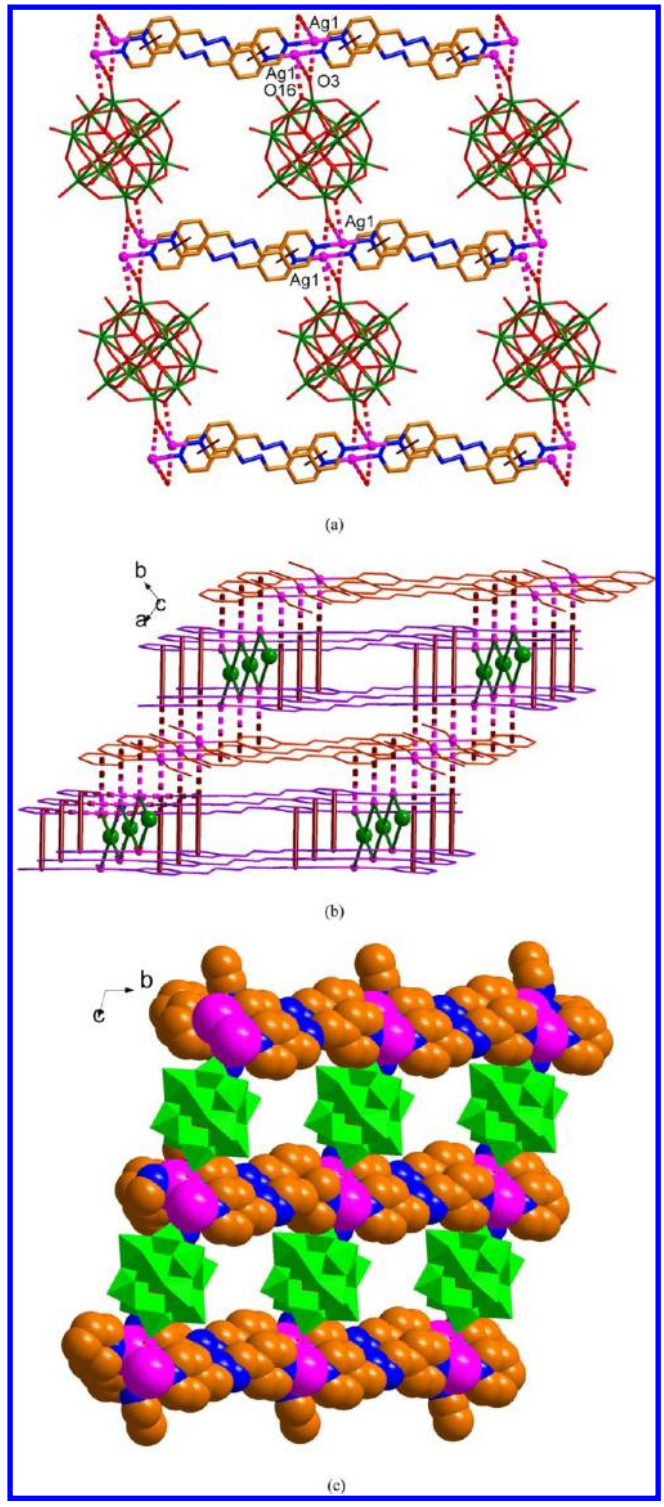

Figure 6. (a) A view of a 2D sheet containing Ag(1)-L^7-chain and $[PMo_{12}O_{40}]^{3-}$ in **6** showing weak Ag···O interactions in dashed lines and $\pi\cdots\pi$ interactions in solid lines. (b) A view of the 3D structure based on two types of 1D Ag(1)-L^7-chain units (purple chains) and Ag(2)-L^7-chain units (orange chains) and $[PMo_{12}O_{40}]^{3-}$ anions (green ball) in **6** showing Ag···π interactions in dashed lines and $\pi\cdots\pi$ interactions in solid lines. (c) A view of the 3D supramolecular network along the *bc* plane in **6**.

Compound **6** crystallizes in a centrosymmetric space group $P\bar{1}$. As shown in Figure 6a, each ligand acts as a bidentate ligand and links two symmetrical Ag(1) or Ag(2) ions through two terminal $N_{pyridyl}$ atoms to form two types of 1D structures [Ag(1)-L^7-chain and Ag(2)-L^7-chain] with the Ag···Ag separations of 15.68 Å and 15.46 Å. The average Ag–$N_{pyridyl}$ distance is 2.17 Å. There are three types of weak Ag···O

dx.doi.org/10.1021/cg300075a | *Cryst. Growth Des.* 2012, 12, 3856–3867

interactions between Ag(1) and three oxygen atoms of two $[PMo_{12}O_{40}]^{3-}$ anions with the distances of 2.79 Å for Ag(1)···O(3), 3.00 Å for Ag(1)···O(16) and 3.08 Å for Ag(1)···O(3), respectively. One terminal oxygen atom O(3) links two Ag(1) atoms with the Ag···Ag separation of 3.61 Å. Accordingly, each $[PMo_{12}O_{40}]^{3-}$ anion interconnects with four Ag(1) centers from four Ag(1)-L^7-chain units through the symmetrical terminal oxygen atoms μ-O(3) and the bridging oxygen atoms O(16) to increase the dimensionality of the compound to form a 2D sheet. The $\pi\cdots\pi$ interaction between pyridyl rings from adjacent Ag(1)-L^7-chain units is found in the 2D structure and characterized by the shortest interplanar atom···atom separation of 3.33 Å, the centroid···centroid separation of 3.77 Å, and the dihedral angle of 8.3°. Detailed structural analyses revealed that the above 2D sheets and Ag(2)-L^7-chain units further interacted with each other featuring a 3D network through the combination of Ag···π interactions and multiform hydrogen bonds (Figure 6b,c). The Ag···π separation is 3.38 Å for Ag(1)···Py[N(5)C(13)−C(17)] and 3.34 Å for Ag(2)···Py[N(1)C(1)−C(5)], respectively.

Structural Analysis in the Self-Assembly Process. Single crystal X-ray diffraction analysis revealed that the structures of **1**−**6** exhibit new crystalline 3D structures based on 1D coordination polymers constructed by the coordination of polydentate Schiff-base ligands and silver cations and saturated α-Keggin polyoxoanion $[PM_{12}O_{40}]^{3-}$ (M = W, Mo) as nanometer-sized anionic clusters. The longer ligands L^4, L^5, L^6, and L^7 with two pyridylimine units linked by a single −N−N− show approximate planar conformation and are favorable to bridge silver ions with *transoid* configuration of two pyridyl rings to form similar 1D chain structures in **1**−**6**. Simultaneously, α-Keggin polyoxoanions of **1**−**6** represent the feature of multiplicity interaction units not only to balance the charge of silver-Schiff base building blocks as larger counteranions, but also to link the silver-Schiff base building blocks through Ag···O interactions as the source of oxygen donors. Apparently, this synthesis of the incorporation of nanometer-sized POMs into silver-Schiff base systems is an excellent strategy to obtain new inorganic−organic hybrid structures and the structure of products can be probed systematically to determine the effect of modifications to the ligand backbone through which we are attempting to control the precise microarchitecture of the arrays. Furthermore, the multiform interaction based on nanometer-sized POMs units is favorable to obtain POM-based frameworks with high rigidity and porosity. This approach has stimulated us to exploit this tendency and to investigate the potential of silver-Schiff base systems acting as secondary building blocks in conjunction with larger POMs to construct 3D porous frameworks.

XRD and BET Measurements. The identical phase of the bulk samples was confirmed by XRD measurements with the most intense peaks observed in the patterns are consistent with those calculated from single-crystal diffraction data (Figures S9 and S10). To prove the porosities of the frameworks, the BET measurements for **1**−**6** have been performed under different conditions, but none of them was successful. This may be due to the existence of plenty of intermolecular interactions which make it very difficult to remove the solvent molecules from the porous under mild conditions.

Photoluminescence. The synthesis of coordination compounds by the judicious choice of conjugated organic ligands and transition metal centers can be an efficient method for obtaining new types of luminescent compounds, especially for d^{10}-metal systems. Among them, the luminescent properties of some metal−organic complexes assembly from Schiff-base ligands have already been investigated previously.[22,30] To enrich the fluorescent database of this type, luminescent emissions of compounds **1**−**6** were investigated in the solid state at room temperature upon excitation at 220 nm (Figure 7). Compound **1** shows luminescent emission maxima at 320 nm, which is comparable to that of the corresponding ligand L^4 (λ_{em} = 326 nm).[31] Compound **2** shows the main emission peaks at 322 and 373 nm. Compounds **3** and **4** have the similar solid-state emission spectra. They show luminescent emission maxima at 326 nm for **3** and 314 nm for **4** when the excitation wavelength is 220 nm. The emission peak of ligand L^5 is at 315 nm. Compared to that of the corresponding ligand L^5, the two compounds both exhibit weaker fluorescence signals, which have been commonly observed in other Schiff base complexes.[30] Compound **5** and ligand L^6 have the same emission peak position at 328 nm, but the intensity of former is slightly weaker than that of the later. Compound **6** and ligand L^7 have the similar emission peak position at 328 and 332 nm, respectively, but the intensity of former is slightly stronger. In summary, the luminescent emissions of the six compounds are all from those of the ligands, which can be ascribed to the intraligand $\pi^*-\pi$ transitions. The distortion of the ligands resulted from their coordination with the metal ions, and the dilution effect of polyoxoanions with the larger size in the compounds may be two of the reasons that make the emissions of complexes get weaker than pure ligands from a structural point of view.

Thermogravimetric (TG) Analyses. Thermogravimetric experiments were conducted to study the thermal stability of compounds **1**−**6**, which is an important parameter of inorganic−organic hybrid materials. The TG properties of **1**−**6** were measured under air atmosphere from 25 to 800 °C (Figure S11). In these six compounds based on POMs, solvent molecules are all participated in structure self-assembly, so the weight loss basically corresponds to the release of solvent molecules below 200 °C. On the other hand, beyond about 600 °C the decomposition of polyoxoanions brings out TG curve decline. Concretely, for **1**, the first weight loss of 2.3% in the range of 42−185 °C corresponds to the release of crystalline H_2O molecules. The second weight loss of 20.04% between 185 and 628 °C is attributed to the loss of two DMF molecules and two ligands (calcd. 20.3%). Finally, the third ligand is lost in a continuous fashion after 628 °C accompanying the decomposition of the polyoxoanion. Similarly, the weight loss of **2** corresponds the loss of crystalline H_2O molecules, three ligands, and decomposition of polyoxoanion. For compound **3**, the weight loss attributed to the gradual release of three CH_3CN molecules, and one ligand is observed in the range from 65 to 330 °C (obsd. 12.4%, calcd. 11.5%). Second, two ligands are lost in a continuous fashion after 330 °C accompanying the decomposition of the polyoxoanion. For **4**, the weight loss of 17.3% in the temperature range of 35−390 °C is due to the release of crystalline and coordinated solvent molecules as well as the ligands (calcd. 16.9%). The compound loses weight rapidly from 610 °C and continues even above 800 °C, indicating the decomposition of polyoxoanion is still processing even at the upper limit of the measurement range. TG curve of **5** exhibits a three-step continuous weight loss attributed to the gradual release of one H_2O molecule, one DMF molecule, and one ligand from 55 to 295 °C (obsd. 12.1%, calcd. 11.2%), other two ligands after 295 °C

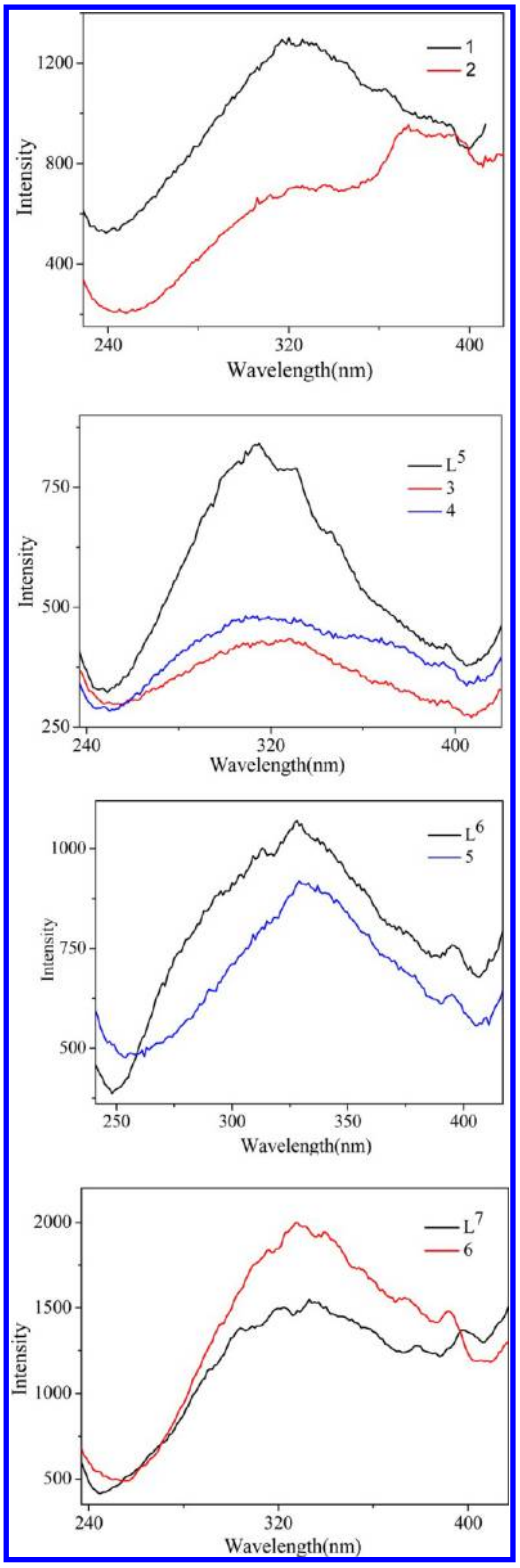

Figure 7. Photoinduced emission spectra of L^5, L^6, L^7, and **1**–**6** in the solid state at room temperature (λ_{ex} = 220 nm).

accompanying the decomposition of the polyoxoanion. For compound **6**, the TG curve also exhibits three continuous weight loss stages corresponding to three CH_3CN molecules in the range of 48–235 °C (obsd. 3.9%, calcd. 4.1%), one DMF molecule, three ligands, and one polyoxoanion. These results show that the thermal stability of such compounds, to a certain extent depending on the property of the ligands, is not very satisfactory, although the decomposition temperatures of polyoxoanions are very high for all six compounds.

CONCLUSIONS

Six new POM-based 3D metal–organic frameworks based on silver(I)-Schiff base coordination polymeric chain species and saturated Keggin type polyoxoanions $[PM_{12}O_{40}]^{3-}$ (M = W, Mo) have been synthesized and complete single-crystal X-ray diffraction analyses. Compounds $\{[AgL^4(DMF)]\text{-}[AgL^4]_2(PMo_{12}O_{40})\cdot DMF\cdot 3H_2O\}_n$ (**1**) and $\{[(AgL^4)_3]\text{-}(PW_{12}O_{40})\cdot 6H_2O\}_n$ (**2**) (L^4 = 2,5-bis(3-pyridyl)-3,4-diaza-2,4-hexadiene) exhibit interesting 3D chiral structures based on three types of 1D Ag-L^4-chain units and $[PMo_{12}O_{40}]^{3-}$ anions for **1**, $[PW_{12}O_{40}]^{3-}$ anions for **2** using the multiform supramolecular interactions of weak Ag···O interactions, weak Ag···N interactions, Ag···π interactions, and hydrogen bonds. Compounds $\{[AgL^5]_3(PMo_{12}O_{40})\cdot(CH_3CN)_3\}_n$ (**3**) and $\{[AgL^5(PW_{12}O_{40})][AgL^5(H_2O)_{0.25}(MeOH)_{0.25})]\text{-}[AgL^5]_{0.5}\cdot DMF\cdot(H_2O)_{1.5}\}_n$ (**4**) (L^5 = 1,4-bis(3-pyridyl)-2,3-diaza-1,3-butadiene) exhibit 3D networks through weak Ag···O interactions, π···π interactions, Ag···π interactions, hydrogen bonds between two types of Ag-L^5-chain units and $[PMo_{12}O_{40}]^{3-}$ anions for **3**, weak Ag···O interactions, π···π interactions, hydrogen bonds between three types of Ag-L^5-chain units and $[PW_{12}O_{40}]^{3-}$ anions for **4**, respectively. Compound $\{[AgL^6]_3(PMo_{12}O_{40})\cdot DMF\cdot H_2O\}_n$ (**5**) (L^6 = 2,5-bis(4-pyridyl)-3,4-diaza-2,4-hexadiene) displays a 3D supramolecular network based on two types of 1D Ag-L^6-chain units and $[PMo_{12}O_{40}]^{3-}$ anions using weak Ag···O interactions, π···π interactions, and hydrogen bonds. Compound $\{[AgL^7]_3(PMo_{12}O_{40}).DMF.(CH_3CN)_3\}_n$ (**6**) (L^7 = 1,4-bis(4-pyridyl)-2,3-diaza-1,3-butadiene) displays a 3D supramolecular network based on two types of 1D Ag-L^7-chain units and $[PMo_{12}O_{40}]^{3-}$ anions using weak Ag···O interactions, π···π interactions, Ag···π interactions, and hydrogen bonds. The successful preparations of **1**–**6** enrich the structural diversity of POM-based compounds and provide us an efficient synthetic strategy for the incorporation of Schiff-base ligands into the POM species to construct POM-based functional MOFs with different topological structures. Studies on the assembly of other types of metal-Schiff base systems and polyoxometalates are currently under way.

ASSOCIATED CONTENT

Supporting Information

Tables of selected bond lengths (Å) and bond angles (deg) for compounds **1**–**6**; some structural figures, luminescent spectra, XRD spectra, and TG data of compounds **1**–**6**. X-ray crystallographic data in CIF format for compounds **1**–**6**. This material is available free of charge via the Internet at http://pubs.acs.org.

AUTHOR INFORMATION

Corresponding Author

*E-mail: baiyan@henu.edu.cn (Y.B.). Tel: 86-378-3881589. Fax: 86-378-3881589. E-mail: jyniu@henu.edu.cn (J.N.).

Notes

The authors declare no competing financial interest.

■ ACKNOWLEDGMENTS

This work was supported by the National Natural Science Foundation of China (No. 21071044), China Postdoctoral Special Science Foundation funded project, China Postdoctoral Science Foundation Funded Project, the Foundation Co-established by the Province and the Ministry of Henan University and the Foundation of Education Department of Henan Province.

■ REFERENCES

(1) (a) Pope, M. T. Polyoxoanions: Synthesis and Structure. *Comprehensive Coordination Chemistry II*; Wedd, A. G., Ed.; Elsevier Science: New York, 2004; Vol. *4*, p 635. (b) *Polyoxometalate Chemistry: From Topology Via Self-Assembly to Applications*; Pope, M. T., Müller, A., Eds.; Kluwer: Dordrecht, The Netherlands, 2001. (c) Hill, C. L. Polyoxometalates: Reactivity. *Comprehensive Coordination Chemistry II*; Wedd, A. G., Ed.; Elsevier Science: New York, 2004; Vol. *4*, p 679.

(2) (a) Dolbecq, A.; Dumas, E.; Mayer, C. R.; Mialane, P. *Chem. Rev.* **2010**, *110*, 6009. (b) Long, D.-L.; Burkholder, E.; Cronin, L. *Chem. Soc. Rev.* **2007**, *36*, 105. (c) Coronado, E.; Gimenez-Saiz, C.; Gomez-Garcia, C. J. *Coord. Chem. Rev.* **2005**, *249*, 1776. (d) Pradeep, C. P.; Long, D.-L.; Cronin, L. *Dalton Trans.* **2010**, *39*, 9443.

(3) (a) Long, D.-L.; Tsunashima, R.; Cronin, L. *Angew. Chem., Int. Ed.* **2010**, *49*, 1736. (b) Zheng, S. T.; Zhang, H.; Yang, G. Y. *Angew. Chem., Int. Ed.* **2008**, *47*, 3909. (c) Sun, C. Y.; Liu, S. X.; Liang, D. D.; Shao, K. Z.; Ren, Y. H.; Su, Z. M. *J. Am. Chem. Soc.* **2009**, *131*, 1883. (d) Ma, F. J.; Liu, S. X.; Sun, C. Y.; Liang, D. D.; Ren, G. J.; Wei, F.; Chen, Y. G.; Su, Z. M. *J. Am. Chem. Soc.* **2011**, *133*, 4178. (e) Kikukawa, Y.; Yamaguchi, K.; Mizuno, N. *Angew. Chem., Int. Ed.* **2010**, *49*, 6096.

(4) (a) Wang, X. L.; Qin, C.; Lan, Y. Q.; Shao, K. Z.; Su, Z. M.; Wang, E. B. *Chem. Commun.* **2009**, 410. (b) Li, C. H.; Huang, K. L.; Chi, Y. N.; Liu, X.; Han, Z. G.; Shen, L.; Hu, C. W. *Inorg. Chem.* **2009**, *48*, 2010. (c) Xiao, F. P.; Hao, J.; Zhang, J.; Lv, C. L.; Yin, P. C.; Wang, L. S.; Wei, Y. G. *J. Am. Chem. Soc.* **2010**, *132*, 5956. (d) Lin, X. K.; Liu, F.; Li, H. L.; Yan, Y.; Bi, L. H.; Bu, W. F.; Wu, L. X. *Chem. Commun.* **2011**, *47*, 10019. (e) Yelamanchili, R. S.; Walther, A.; Müller, A. H. E.; Breu, J. *Chem. Commun.* **2008**, 489.

(5) (a) Uchida, S.; Eguchi, R.; Mizuno, N. *Angew. Chem., Int. Ed.* **2010**, *49*, 9930. (b) Zhou, J.; Zhang, J.; Fang, W. H.; Yang, G. Y. *Chem.—Eur. J.* **2010**, *16*, 13253. (c) Arumuganathan, T.; Rao, A. S.; Das, S. K. *Cryst. Growth Des.* **2010**, *10*, 4272. (d) Tian, A. X.; Ying, J.; Peng, J.; Sha, J. Q.; Su, Z. M.; Pang, H. J.; Zhang, P. P.; Chen, Y.; Zhu, M.; Shen, Y. *Cryst. Growth Des.* **2010**, *10*, 1104.

(6) (a) Ritchie, C.; Moore, E. G.; Speldrich, M.; Kögerler, P.; Boskovic, C. *Angew. Chem., Int. Ed.* **2010**, *49*, 7702. (b) Hou, G. F.; Bi, L. H.; Li, B.; Wang, B.; Wu, L. X. *CrystEngComm* **2011**, *13*, 3526. (c) Xiao, L. N.; Wang, Y.; Pan, C. L.; Xu, J. N.; Wang, T. G.; Ding, H.; Gao, Z. M.; Zheng, D. F.; Cui, X. B.; Xu, J. Q. *CrystEngComm* **2011**, *13*, 4878. (d) Wang, X. L.; Bi, Y. F.; Chen, B. K.; Lin, H. Y.; Liu, G. C. *Inorg. Chem.* **2008**, *47*, 2442.

(7) (a) Kong, X. J.; Ren, Y. P.; Zheng, P. Q.; Long, Y. X.; Long, L. S.; Huang, R. B.; Zheng, L. S. *Inorg. Chem.* **2006**, *45*, 10702. (b) Zhang, P. P.; Peng, J.; Pang, H. J.; Sha, J. Q.; Zhu, M.; Wang, D. D.; Liu, M. G. *CrystEngComm* **2011**, *13*, 3832. (c) Dang, D. B.; Bai, Y.; He, C.; Wang, J.; Duan, C. Y.; Niu, J. Y. *Inorg. Chem.* **2010**, *49*, 1280. (d) Putaj, P.; Lefebvre, F. *Coord. Chem. Rev.* **2011**, *255*, 1642.

(8) (a) McGlone, T.; Streb, C.; Busquets-Fité, M.; Yan, J.; Gabb, D.; Long, D.-L.; Cronin, L. *Cryst. Growth Des.* **2011**, *11*, 2471. (b) Wilson, E. F.; Abbas, H.; Duncombe, B. J.; Streb, C.; Long, D.-L.; Cronin, L. *J. Am. Chem. Soc.* **2008**, *130*, 13876. (c) Abbas, H.; Streb, C.; Pickering, A. L.; Neil, A. R.; Long, D.-L.; Cronin, L. *Cryst. Growth Des.* **2008**, *8*, 635. (d) Streb, C.; Ritchie, C.; Long, D.-L.; Kögerler, P.; Cronin, L. *Angew. Chem., Int. Ed.* **2007**, *46*, 7579. (e) Song, Y. F.; Abbas, H.; Ritchie, C.; McMillian, N.; Long, D.-L.; Gadegaard, N.; Cronin, L. *J. Mater. Chem.* **2007**, *17*, 1903.

(9) (a) Sha, J. Q.; Peng, J.; Lan, Y. A.; Su, Z. M.; Pang, H. J.; Tian, A. X.; Zhang, P. P.; Zhu, M. *Inorg. Chem.* **2008**, *47*, 5145. (b) Sha, J. Q.; Peng, J.; Li, Y. G.; Zhang, P. P.; Pang, H. J. *Inorg. Chem. Commun.* **2008**, *11*, 907. (c) Pang, H. J.; Peng, J.; Sha, J. Q.; Tian, A. X.; Zhang, P. P.; Chen, Y.; Zhu, M. *J. Mol. Struct.* **2009**, *921*, 289. (d) Han, Z. G.; Zhao, Y. L.; Peng, J.; Ma, H. Y.; Liu, Q.; Wang, E. B.; Hu, N. H.; Jia, H. Q. *Eur. J. Inorg. Chem.* **2005**, 264.

(10) (a) Li, S. L.; Lan, Y. Q.; Ma, J. F.; Yang, J.; Wang, X. H.; Su, Z. M. *Inorg. Chem.* **2007**, *46*, 8283. (b) Gao, G. G.; Cheng, P. S.; Mak, T. C. W. *J. Am. Chem. Soc.* **2009**, *131*, 18257. (c) Zhao, X. L.; Mak, T. C. W. *Inorg. Chem.* **2010**, *49*, 3676. (d) Nogueira, H. I. S.; Almeida Paz, F. A.; Teixeira, P. A. F.; Klinowski, J. *Chem. Commun.* **2006**, 2953. (e) Duval, S.; Pilette, M.-A.; Marrot, J.; Simonnet-Jégat, C.; Sokolov, M.; Cadot, E. *Chem.—Eur. J.* **2008**, *14*, 3457. (f) Zhai, Q. G.; Wu, X. Y.; Chen, S. M.; Zhao, Z. G.; Lu, C. Z. *Inorg. Chem.* **2007**, *46*, 5046.

(11) (a) Yuan, L.; Qin, C.; Wang, X. L.; Li, Y. G.; Wang, E. B. *Dalton Trans.* **2009**, 4169. (b) Chen, J.; Sha, J. Q.; Peng, J.; Shi, Z. Y.; Tian, A. X.; Zhang, P. P. *J. Mol. Struct.* **2009**, *917*, 10.

(12) (a) Dai, L. M.; You, W. S.; Wang, E. B.; Wu, S. X.; Su, Z. M.; Du, Q. H.; Zhao, Y.; Fang, Y. *Cryst. Growth Des.* **2009**, *9*, 2110. (b) Luan, G. Y.; Li, Y. G.; Wang, S. T.; Wang, E. B.; Han, Z. B.; Hu, C. W.; Hu, N. H.; Jia, H. Q. *Dalton Trans.* **2003**, 233.

(13) (a) Yang, H. X.; Gao, S. Y.; Lü, J.; Xu, Bo.; Lin, J. X.; Cao, R. *Inorg. Chem.* **2010**, *49*, 736. (b) Sha, J. Q.; Peng, J.; Pang, H. J.; Tian, A. X.; Chen, J.; Zhang, P. P.; Zhu, M. *Solid State Sci.* **2008**, *10*, 1491. (c) Chen, J. X.; Lan, T. Y.; Huang, Y. B.; Wei, C. X.; Li, Z. S.; Zhang, Z. C. *J. Solid State Chem.* **2006**, *179*, 1904.

(14) Ren, Y. P.; Kong, X. J.; Long, L. S.; Huang, R. B.; Zheng, L. S. *Cryst. Growth Des.* **2006**, *6*, 572.

(15) (a) Yang, M. X.; Lin, S.; Chen, L. J.; Zhang, X. F.; Xu, H. H. *Inorg. Chem. Commun.* **2009**, *12*, 566. (b) Lü, J.; Xiao, F. X.; Shi, L. X.; Cao, R. *J. Solid State Chem.* **2008**, *181*, 313. (c) Pang, H. J.; Chen, J.; Peng, J.; Sha, J. Q.; Shi, Z. Y.; Tian, A. X.; Zhang, P. P. *Solid State Sci.* **2009**, *11*, 824.

(16) Lan, Y. Q.; Li, S. L.; Shao, K. Z.; Wang, X. L.; Su, Z. M. *Dalton Trans.* **2008**, 3824.

(17) Dang, D. B.; Gao, H.; Bai, Y.; Hu, X. F.; Yang, F.; Niu, J. Y. *Inorg. Chem. Commun.* **2010**, *13*, 37.

(18) Dang, D. B.; Zheng, G. S.; Bai, Y.; Yang, F.; Gao, H.; Ma, P. T.; Niu, J. Y. *Inorg. Chem.* **2011**, *50*, 7907.

(19) Bai, Y.; Zhang, G. Q.; Dang, D. B.; Ma, P. T.; Gao, H.; Niu, J. Y. *CrystEngComm* **2011**, *13*, 4181.

(20) (a) He, C.; Zhao, Y. G.; Guo, D.; Lin, Z. H.; Duan, C. Y. *Eur. J. Inorg. Chem.* **2007**, 3451. (b) Tuna, F.; Clarkson, G.; Alcock, N. W.; Hannon, M. J. *Dalton Trans.* **2003**, 2149. (c) Guo, D.; Pang, K. L.; Duan, C. Y.; He, C.; Meng, Q. J. *Inorg. Chem.* **2002**, *41*, 5978.

(21) (a) Wu, Q.; Li, Y. G.; Wang, Y. H.; Clérac, R.; Lu, Y.; Wang, E. B. *Chem. Commun.* **2009**, 5743. (b) Wei, M. L.; Sun, R. P.; Zhuang, P. F.; Yang, Y. H. *Russ. J. Coord. Chem.* **2009**, *35*, 885.

(22) (a) Bai, Y.; Gao, H.; Dang, D. B.; Guo, X. Y.; An, B.; Shang, W. L. *CrystEngComm* **2010**, *12*, 1422. (b) Dang, D. B.; Zheng, G. S.; Bai, Y. *J. Inorg. Organomet. Polym. Mater.* **2010**, *20*, 356. (c) Dang, D. B.; Gao, H.; Bai, Y.; Pan, X. J.; Shang, W. L. *J. Mol. Struct.* **2010**, *969*, 120. (d) Dang, D. B.; Li, M. M.; Bai, Y.; Wang, J. L. *Spectrochim. Acta, Part A* **2011**, *83*, 499.

(23) (a) Bai, Y.; Zheng, G. S.; Dang, D. B.; Gao, H.; Qi, Z. Y.; Niu, J. Y. *Spectrochim. Acta, Part A* **2010**, *77*, 727. (b) Dang, D. B.; Fan, Y. H.; Bai, Y.; Jin, Y. N. *Synth. React. Inorg., Met.-Org., Nano-Met. Chem.* **2010**, *40*, 748. (c) Dang, D. B.; Gao, H.; Bai, Y.; Jin, Y. N.; Sun, J. D.; Niu, J. Y. *Chin. J. Struct. Chem.* **2010**, *29*, 151.

(24) (a) McHugh, C. J.; Murdoch, P.; Smith, W. E. *New J. Chem.* **2005**, *29*, 826. (b) Dong, Y. B.; Smith, M. D.; Loye, H. C. Z. *Inorg. Chem.* **2000**, *39*, 4927.

(25) (a) Mahmoudi, G.; Morsali, A.; Hunterb, A. D.; Zellerb, M. *CrystEngComm* **2007**, *9*, 704. (b) Mahmoudi, G.; Morsali, A. *CrystEngComm* **2009**, *11*, 50. (c) Khanpour, M.; Morsali, A. *CrystEngComm* **2009**, *11*, 2585. (d) Bigdeli, F.; Morsali, A.; Retailleau, P. *Polyhedron* **2010**, *29*, 801. (e) Ross, T. M.; Neville, S. M.; Innes, D. S.; Turner, D. R.; Moubaraki, B.; Murray, K. S. *Dalton*

Trans. **2010**, *39*, 149. (f) Wang, Q.; Yang, R.; Zhuang, C. F.; Zhang, J. Y.; Kang, B. S.; Su, C. Y. *Eur. J. Inorg. Chem.* **2008**, 1702.
(26) (a) Gao, E. Q.; Cheng, A. L.; Xu, Y. X.; Yan, C. H.; He, M. Y. *Cryst. Growth Des.* **2005**, *5*, 1005. (b) Kennedy, A. R.; Brown, K. G.; Graham, D.; Kirkhouse, J. B.; Kittner, M.; Major, C.; McHugh, C. J.; Murdoch, P.; Smith, W. E. *New J. Chem.* **2005**, *29*, 826. (c) Chen, M. S.; He, C. M.; Deng, Y. F.; Kuang, D. Z.; Zhang, C. H.; Deng, W. Y. *Chin. J. Inorg. Chem.* **2009**, *25*, 1312.
(27) Claude, R. D.; Michael, F.; Raymonde, F.; Rene, T. *Inorg. Chem.* **1983**, *22*, 207.
(28) Sheldrick, G. M. *Acta Crystallogr., Sect. A* **1998**, *46*, 467.
(29) Sheldrick, G. M. *SHELXL-97, Programs for Crystal Structure Analysis*; University of Göttingen: Germany, 1997.
(30) (a) Wu, H. C.; Thanasekaran, P.; Tsai, C. H.; Wu, J. Y.; Huang, S. M.; Wen, Y. S.; Lu, K. L. *Inorg. Chem.* **2006**, *45*, 295. (b) Dong, Y. B.; Wang, L.; Ma, J. P.; Zhao, X. X.; Shen, D. Z.; Huang, R. Q. *Cryst. Growth Des.* **2006**, *6*, 2475.
(31) Dang, D. B.; Guo, X. Y.; Bai, Y.; Gao, H.; Zhang, G. Q. *Synth. React. Inorg., Met.-Org., Nano-Met. Chem.* **2010**, *40*, 195.